Article

Discovery of Novel α-Carboline Inhibitors of the Anaplastic Lymphoma Kinase

Luca Mologni,*,[¶] Sébastien Tardy,[¶] Alfonso Zambon, Alexandre Orsato, William H. Bisson, Monica Ceccon, Michela Viltadi, Joseph D'Attoma, Sara Pannilunghi, Vito Vece, Jerome Bertho, Peter Goekjian,[¶] Leonardo Scapozza,*,[¶] and Carlo Gambacorti-Passerini[¶]

ACCESS | 📊 Metrics & More | 📖 Article Recommendations | 🔲 Supporting Information

ABSTRACT: The anaplastic lymphoma kinase (ALK) is abnormally expressed and hyperactivated in a number of tumors and represents an ideal therapeutic target. Despite excellent clinical responses to ALK inhibition, drug resistance still represents an issue and novel compounds that overcome drug-resistant mutants are needed. We designed, synthesized, and evaluated a large series of azacarbazole inhibitors. Several lead compounds endowed with submicromolar potency were identified. Compound **149** showed selective inhibition of native and mutant drug-refractory ALK kinase *in vitro* as well as in a Ba/F3 model and in human ALK+ lymphoma cells. The three-dimensional (3D) structure of a **149**:ALK-KD cocrystal is reported, showing extensive interaction through the hinge region and the catalytic lysine 1150.
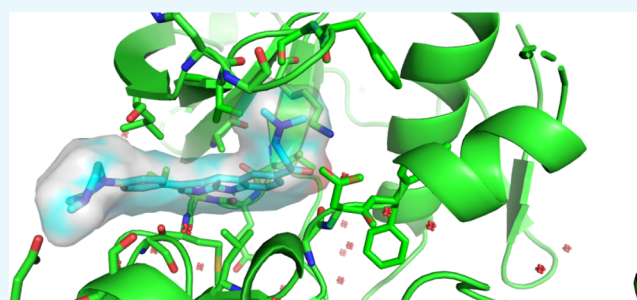
1. INTRODUCTION

Anaplastic lymphoma kinase (ALK) is rearranged or mutated in several cancers of different origins.[1] About 50−80% of anaplastic large-cell lymphoma (ALCL) cases express the nucleophosmin (NPM)-ALK or other fusion proteins involving the catalytic domain of ALK. Rearrangements have also been identified in approximately 50% of patients affected by inflammatory myofibroblastic tumor (IMT), 3−8% of nonsmall cell lung cancer (NSCLC) patients, as well as in rare cases of other cancer types, including leukemia, melanoma, breast, and colorectal carcinoma. In addition, activating point mutations are found in sporadic and familial neuroblastoma. Whatever the type of abnormality, all ALK-positive tumors show high expression and constitutive ligand-independent activation of the tyrosine kinase activity derived from the ALK gene, which dictates aberrant intracellular signaling leading to enhanced cell proliferation and survival.

Small-molecule-mediated inhibition of ALK kinase activity has shown excellent clinical results in ALCL and NSCLC patients.[2,3] The first-generation inhibitor crizotinib has been in clinical use since 2011 and has changed the therapeutic paradigm in these patients. Unfortunately, however, responses are often short-lived, in particular in the NSCLC population, probably due to the high genetic heterogeneity of the advanced disease and the selection of subclonal mutants that are resistant to the drug. Second and third-generation ALK inhibitors have been developed to tackle the problem of drug resistance.[1] However, the use of more potent inhibitors has driven the rise of compound mutants.[4−6] Therefore, a continuous search for new

compounds with different activity profiles on ALK mutants is underway, with several new molecules on the horizon.

We started a rational drug design program with the aim to identify novel compounds with unconventional binding modes within the ALK active site. Starting from the published crystal structures of ALK in complex with several inhibitors, we used molecular modeling to dock drug-like compounds from publicly available databases. Top scoring virtual hits were experimentally tested for ALK kinase inhibition, providing active micromolar hits that were used as starting models to design new ALK inhibitors. Herein, we present our medicinal chemistry effort leading to the identification of new lead candidates for preclinical optimization.

2. CHEMISTRY

Target compounds were synthesized starting from the appropriate benzenesulfonyl-protected halogenated pyrido-[2,3-b]indole by sequential palladium-catalyzed couplings followed by deprotection, according to Scheme 1. A detailed description of compound synthesis has been reported previously in a patent application[7] and is summarized in the Supporting

Scheme 1. Preparation of Candidate Compounds by Derivatization of α-Carbolines at 2, 3, and 6 Positions
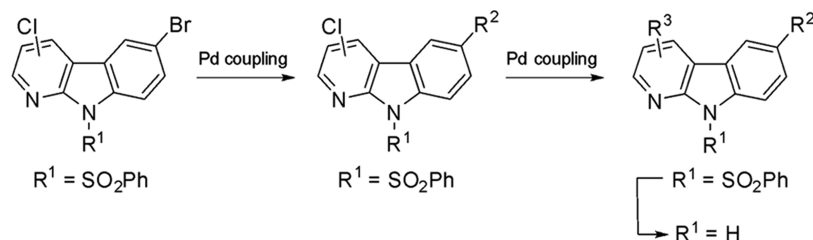
Table 1. Structure and Activity (IC_{50}) of Compounds 1−23

	R1	R2	IC_{50} ALK (μM)
1	H	H	>100
2	H	5-OMe	>100
3	H	6-Ac	>100
4	H	6-CHO	>100
5	H	6-COOH	>100
6	H	6-NH2	>100
7	H	7-OMe	>100
8	H	8-OMe	>100
9	H	6-NO2	10
10	H	6-Br	4.3
11	H	8-Cl	11
12	H	8-NO2	9.2
13	H	6-CO-Ph	42
14	2-Cl	H	18
15	3-Cl	H	9.0
16	4-Cl	H	28
17	2-Me	H	27
18	2,4-Cl	H	1.6
19	4-Cl	8-OMe	56
20	4-Cl	7-OMe	>100
21	2-Me	6-NO2	7.7
22	3-Cl	6-Br	1.7
23	3-Cl	6-CHO	20

Information. All compounds are >95% pure by NMR and high-resolution mass spectrometry (HR-MS) analysis.

3. RESULTS AND DISCUSSION

To identify suitable hit material for the development of novel ATP-competitive ALK inhibitors, we ran a high throughput in silico virtual screening of commercial compound libraries on a number of available ALK three-dimensional (3D) structures: considering kinase plasticity, compounds were docked against several DFG-in ALK cocrystal structures to account for possible different conformations of the enzyme, leading to alternative ligand binding modes within the ATP pocket (see section 5 for details). Virtual hits were tested for recombinant ALK inhibition using an in vitro kinase assay,[8] and a number of micromolar hits were identified (Supporting Table S1). Among these, a recurring chemotype consisted of a fused three-ring system comprising either a fluorene, carbazole, or azacarbazole moiety (entries L−

M, P−Q, S−T in Supporting Table S1). We deemed the α-carboline (1-azacarbazole) structure (Scheme 1) worth exploring for the development of potential lead compounds because of its predicted lower lipophilicity and higher solubility; in addition, the presence of two nitrogen atoms provides the potential to form additional hydrogen bonds with the protein: according to the literature, the α-carboline scaffold should mimic the adenine ring of ATP and behave as a hinge binding motif.[9] Indeed, docking analyses and molecular dynamics simulations predicted that azacarbazole compounds bind within the active site in the DFG-in conformation as a type I inhibitor, making two H-bonds with the hinge backbone, although two alternative docking poses were identified depending on the substitutions around the ligand core (Supporting Figure S1). We then set up to explore how the decoration of the azacarbazole core affects activity on ALK by synthesizing several analogues substituted either on the pyridine or the phenyl ring of the

Table 2. Structure and Activity (IC$_{50}$) of 2,6-Substituted Compounds 24−45
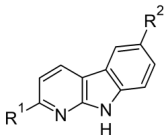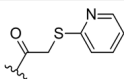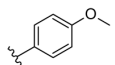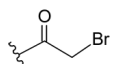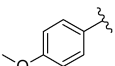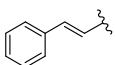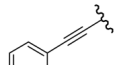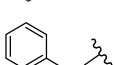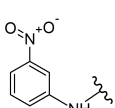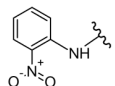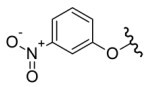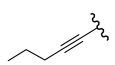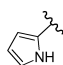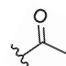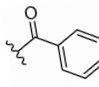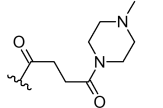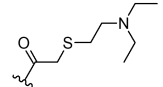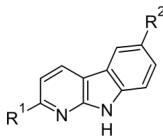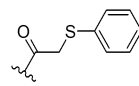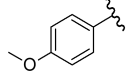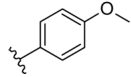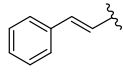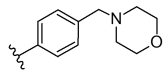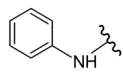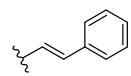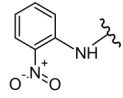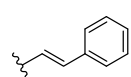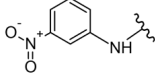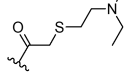
	R^1	R^2	IC$_{50}$ ALK (μM)
24	-H		>10
25	-H		2.9
26	-H		1.8
27		-H	2.1
28		-H	1.2
29		-H	4.1
30		-H	>10
31		-H	8.2
32		-H	4.7
33		-H	>10
34		-H	>10
35		-H	>10
36	-CH$_3$		>10
37	-CH$_3$		>10
38	-Cl		>10
39	-Cl		>10

C

Table 2. continued

	R^1	R^2	IC$_{50}$ ALK (μM)
40	-Cl	phenylthio-acetyl	0.8
41	methoxyphenyl	methoxybenzyl	3.2
42	cinnamyl	benzyl-morpholine	>10
43	phenyl-NH	styryl	2.8
44	2-nitrophenyl-NH	styryl	>10
45	3-nitrophenyl-NH	thioethyl-diethylamine acetyl	>10

azacarbazole core. Compounds were tested *in vitro* using recombinant ALK kinase, and half-maximal inhibitory concentration (IC$_{50}$) is reported (Table 1). It should be noted that the assays were run in the presence of 300 μM ATP to force the selection of high-affinity compounds: given the apparent Km of the purified kinase in our assay (30 μM), K_i values are deemed to be roughly 10-fold lower than IC$_{50}$ values. We observed that substitution on the phenyl ring with carboxy, amino, or methoxy groups yielded only inactive compounds (compounds 1−8), but compounds bearing a halogen or a nitro group in position 6 or 8 (compounds 9−12) already showed micromolar activities on ALK in *in vitro* kinase assays, while ketone 13, also substituted on the 6 position, has lower activity. Compound 10, in particular, inhibited ALK at 4.3 μM, suggesting that substitution on the 6 position is particularly promising to confer potency to the scaffold. The pyridine ring seems more tolerant to substitution, as activities ranging from ∼30 to ∼10 μM were obtained by introducing chloro- or methyl-groups in each position of the ring (compounds 14−17). Furthermore, bis-substituted compound 18 shows a further increase in activity (1.6 μM). When combined, substitutions on both the phenyl and the pyridine ring confirmed a low activity of methoxy-substituted compounds (compounds 19−20) but yielded low-micromolar 2,6- and 3,6-substituted inhibitors 21−23, with the bis-halogen 22 being particularly potent at 1.7 μM. Thus, simple decorations in positions 2, 3, 4, and 6 yielded hit compounds with low-micromolar activity in *in vitro* kinase assays (Table 1).

We then deemed double substitutions on the 2,6 and 3,6 positions worth exploring in more depth (Table 2−4). When evaluating 2,6 compounds (Table 2), we noticed that a single substitution on the 6 position with bromoacetyl or anisole function yielded active compounds 25 and 26. On the other hand, single substitution on position 2 yields active compounds with substituents containing aromatic or conjugated aromatic groups (compounds 27−29) with *trans*-styrene 28 particularly potent at 1.2 μM. Aniline and phenol substituents (compounds

30−33) are not well tolerated, with only *o*- and *m*-nitroanilines 31 and 32 showing hints of activity. Non-benzene compounds 34 and 35 are also inactive, highlighting a tight structure−activity relationship (SAR) in this position. We then investigated the activity of disubstituted compounds starting from small methyl or chloro groups on position 2: within this miniseries, carbonyl substituents on the 6 position (compounds 36−40) were inactive, with the notable exception of 40 which shows submicromolar activity by combining a chloro substituent with a phenylthiol-acetyl group. Further elaboration confirmed good activity of compounds with methoxy-phenyl groups (compound 41; compared with 25 and 27). However, these compounds were not active in intact cells, suggesting that they lacked cell membrane permeability. The styryl moiety showed variable results depending on the context (see compounds 42−44, compared to 28).

Next, we set out to explore the 3,6 pattern focusing initially on 3-chloro-substituted compounds, as it is synthetically more accessible and preliminary 3-chloro compounds did show good activity (Table 1); this approach allowed us to explore a range of substituents on the 6 position with limited synthetic effort. We first synthesized a series of analogues bearing the promising α-thioacetyl pattern (compounds 46−55; Table 3), while compounds with aliphatic substituents on the sulfur showed only marginal activity (compounds 52−54), some of the analogues with aromatic groups did indeed show remarkable activity, with benzothiazole 47 and *m*-bromophenyl 50 showing submicromolar IC$_{50}$ at 0.4 and 0.8 μM, respectively. In analogy with what was observed for the 2,6 series, other 6-carbonyl-substituted compounds (56−62) show generally lower activity toward ALK, with only 2-chloro-acetyl compound 58 showing low-micromolar activity. Among the aromatic and conjugated substitutions (63−71), the activity conferred by the styryl substitution is confirmed, with 63 showing 0.5 μM inhibition against ALK. The anisole substituent (65; 0.8 μM) is significantly more active than its phenol (64) and benzyl

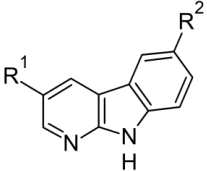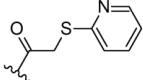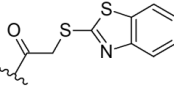**Table 3. Structure and Activity (IC_{50}) of 3-Chloro-6-Substituted Compounds 46−81**
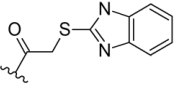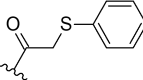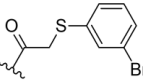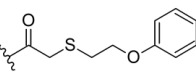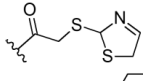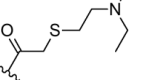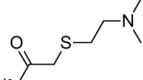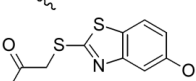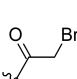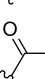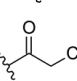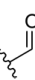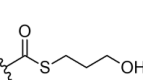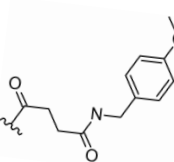
	R^1	R^2	IC_{50} ALK (μM)
46	Cl		7.9
47	Cl		0.4
48	Cl		6.3
49	Cl		2
50	Cl		0.8
51	Cl		1.4
52	Cl		7
53	Cl		6.8
54	Cl		>10
55	Cl		>10
56	Cl		9.7
57	Cl		6.6
58	Cl		1.5
59	Cl		19
60	Cl		7.4
61	Cl		5.1

Table 3. continued
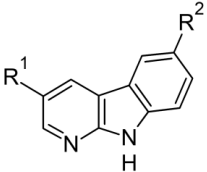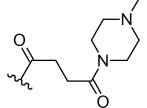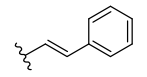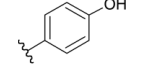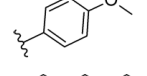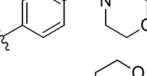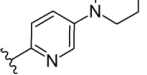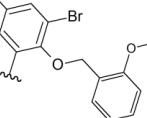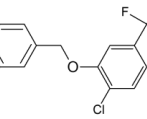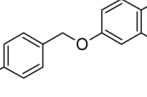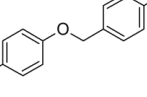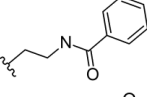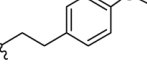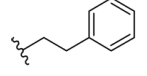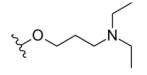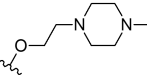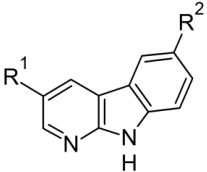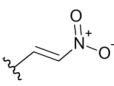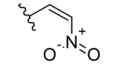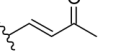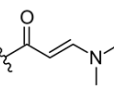
	R^1	R^2	IC$_{50}$ ALK (μM)
62	Cl		>10
63	Cl		0.5
64	Cl		19
65	Cl		0.8
66	Cl		8.8
67	Cl		>10
68	Cl		5.3
69	Cl		3.5
70	Cl		2.0
71	Cl		>10
72	Cl		>10
73	Cl		5.1
74	Cl		>10
75	Cl		>10
76	Cl		7.8

Table 3. continued

	R^1	R^2	IC$_{50}$ ALK (μM)
77	Cl	(trans-nitrovinyl)	3.3
78	Cl	(cis-nitrovinyl)	1.9
79	Cl	(α,β-unsaturated methyl ketone)	1.6
80	Cl	(dimethylamino enone)	>10

morpholino (**66**) analogues, while pyridino compound **67** is inactive. Further elaboration of the phenyl scaffold (compounds **68−71**) does not yield any improvement in activity, with benzyl ethers **69** and **70** slightly more active than phenols **68** and **71**. Switching to aliphatic substitution (compounds **72−74**) or to aliphatic phenol ethers (compounds **75−76**) leads to compounds with no or marginal activity. We finally explored a range of Michael acceptors (compounds **77−80**) as potential mechanistic inhibitors of ALK; interestingly, nitrovynyl compounds **77** and **78** and α,β-unsaturated ketone **79** all show low-micromolar activities. This exploration allowed us to develop an initial QSAR model, with good correlation between expected and experimentally observed IC$_{50}$ values (Supporting Figure S2).

We then combined a range of the most promising substitutions on the 3 and 6 positions to identify compounds both potent and cell permeable (Table 4). First, alternative substitutions on the 3 position with a range of aromatic groups (compounds **81−86**) allowed to identify submicromolar p-tolyl-substituted **83** and confirmed the potency of styryl-substituted compounds with **86** (0.34 μM). Thus, we focused on exploring inhibitors bearing the advantageous styryl group on the 6 (**90−101**) or the 3 (**100−136**) position. As expected, the unsaturation of the ethyl group is essential for activity, as confirmed by inactive ethylbenzene analogues **87−89**. In accordance with our model, 6-styryl-substituted 3-nitrobenzene **90** (1.9 μM) and 3-anisole **91** (2.2 μM) show low-micromolar activities. Further elaboration of the group in 3 position with benzyl ethers **92−99** is tolerated but not beneficial, yielding compounds in the micromolar range. Inhibitors with the styryl group on the 3 position were generally more potent than their 6-styryl analogues, with several compounds showing nanomolar activity against ALK. Unsubstituted **86** (340 nM) remains the most potent compound of the series, although it is completely inactive in cells (not shown); para- (**100−115**) and meta-substituted (**116−121**) aromatic rings on the 6 position provided several active analogues, among which compounds **100**, **106**, **112**, and **120** (the latter two bearing an N-methylpiperazine moiety) showed submicromolar potencies. Conversely, o-substituted compounds (**122−126**) are not particularly active with the exception of ethoxy compound **126** (1.5 μM). We finally explored the effect of multiple substitutions on the substituent on the 6 position. o-Phenyl ethers have micromolar activity if the o-substituent is a benzyl group (cpds **127−129**), while methoxy **130** is inactive. Similarly, difluoro- compounds are again more active if the substituent is an o-benzyl ether (**131−132**) and less active when the substituent is methoxy (**133−134**). Also, elaboration on the 3-styrene subunit is not tolerated, with fluoro and methoxy compounds **135−140** showing little or no activity.

Given the promising activity shown by compounds **25** and **65**, a small subseries of compounds bearing an anisole group on the 6 position (compounds **138−144**) was evaluated. Only the potent bis-anisole **141** showed inhibition in the submicromolar range (0.74 μM). Interestingly, in a clear piece of SAR, switching three substituents from o- to m-substituted styrene (see compounds **138** vs **139−140**) and from nitrobenzene to anilines (**142** vs **143−144**) completely abrogates activity.

Finally, to improve the solubility of the series, which had caused issues for many compounds, we explored a number of analogues carrying the N′-methyl-N-phenyl-piperazine group at the 3 position (compounds **145−149**); intriguingly, compounds **146**, **147**, and **149**, all bearing Michael acceptors on the 6 position, have sub- or low-micromolar activity against ALK, while the other analogues are inactive.

In summary, this series provided several submicromolar ALK inhibitors. Importantly, several compounds from this group also inhibited ALK-dependent cell growth. In particular, compounds **102**, **105**, **106**, and **149** showed selective inhibition of Ba/F3 NPM/ALK cell proliferation compared to parental IL3-dependent Ba/F3 cells (Table 5). More detailed analysis showed that, in addition to wild-type ALK, compound **149** inhibited the L1196M, C1156Y, R1275Q, and F1174L crizotinib-resistant ALK mutants in vitro (Figure 1A and Table 6). The proliferation of Ba/F3 cells expressing NPM/ALK^{L1196M}, but not NPM/ALK^{G1202R}, was inhibited (Table 6). The compound suppressed NPM/ALK phosphorylation and cell growth of human ALK+ ALCL cells (Figure 1B,C and Table 6). Additional in vitro profiling revealed that **149** also inhibits other tyrosine kinases with similar potency, including RET, FLT3, VEGFR2, FGFR2, TRK-A, and TRK-C (Supporting Table S2). On ALK, compound **149** showed ATP-competitive inhibition in biochemical assays (Figure 1D). To gain insights into the binding mode of the compound within the kinase, the

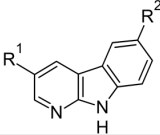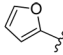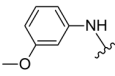**Table 4. Structure and Activity (IC$_{50}$) of 3,6-Substituted Compounds 81−149**
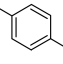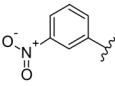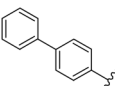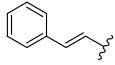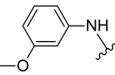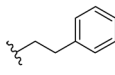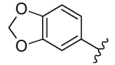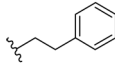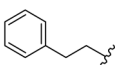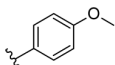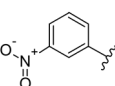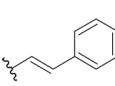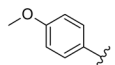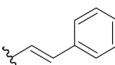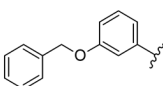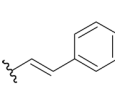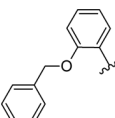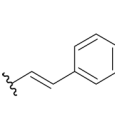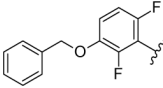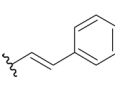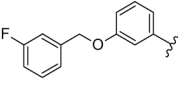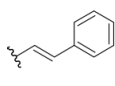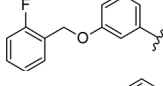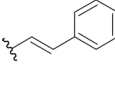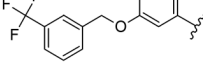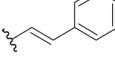
	R^1	R^2	IC$_{50}$ ALK (µM)
81		H	>10
82		H	>10
83		H	1.2
84		H	>10
85		H	>10
86		H	0.34
87			>10
88			>10
89			>10
90			1.9
91			2.2
92			5.2
93			6.7
94			8.7
95			3.3
96			3.2
97			7.5

Table 4. continued
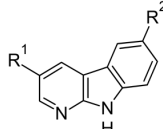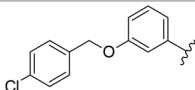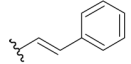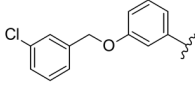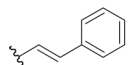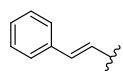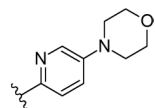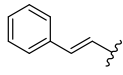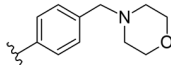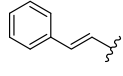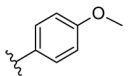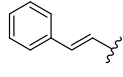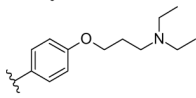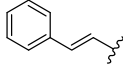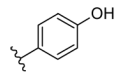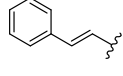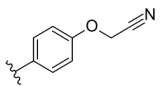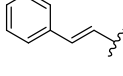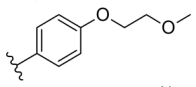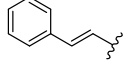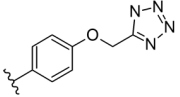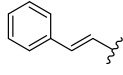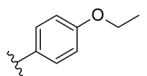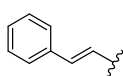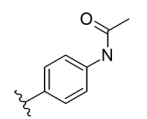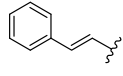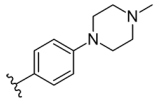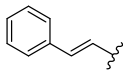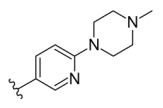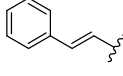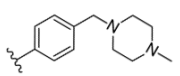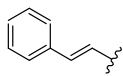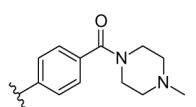
	R^1	R^2	IC$_{50}$ ALK (µM)
98			3.0
99			4.4
100			0.45
101			2.9
102			1.2
103			7.0
104			1.3
105			1.1
106			0.57
107			1.6
108			4.2
109			>10
110			1.6
111			1.6
112			0.97
113			1.4

Table 4. continued
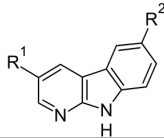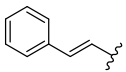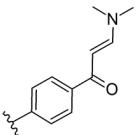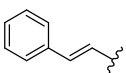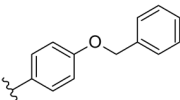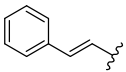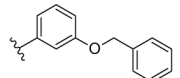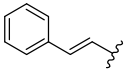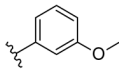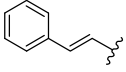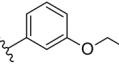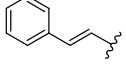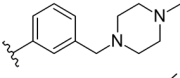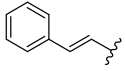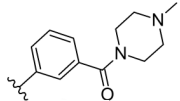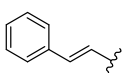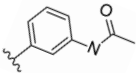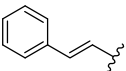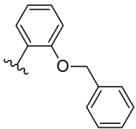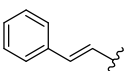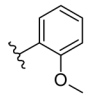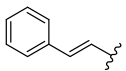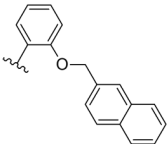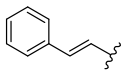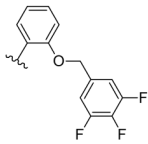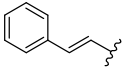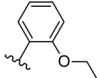
	R¹	R²	IC₅₀ ALK (μM)
114			>10
115			>10
116			5.4
117			>10
118			1.9
119			2.4
120			0.78
121			>10
122			>10
123			8.8
124			2.3
125			2.9
126			1.5

Table 4. continued
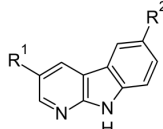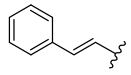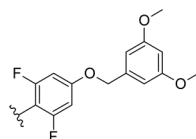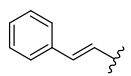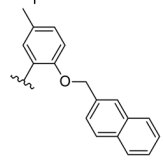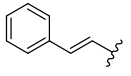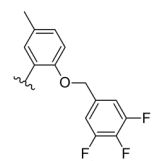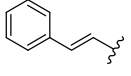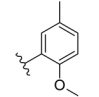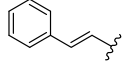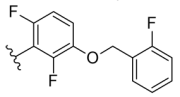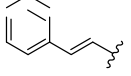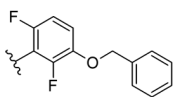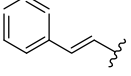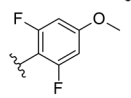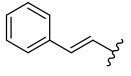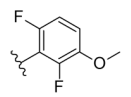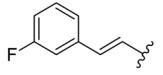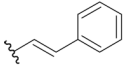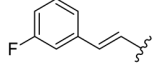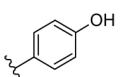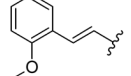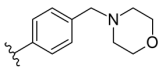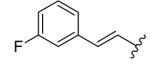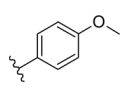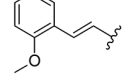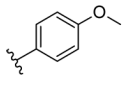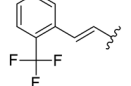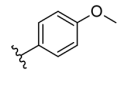
	R¹	R²	IC$_{50}$ ALK (µM)
127			4.2
128			3.1
129			2.9
130			>10
131			1.5
132			0.94
133			3.5
134			4.8
135			>10
136			>10
137			>10
138			>10
139			7.4
140			8.3

Table 4. continued
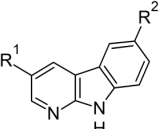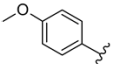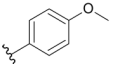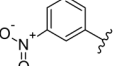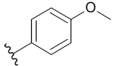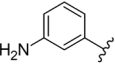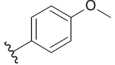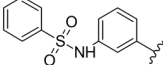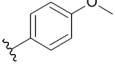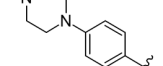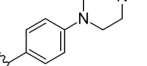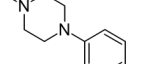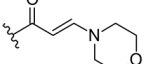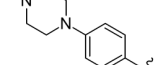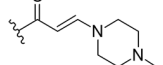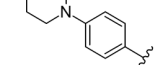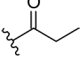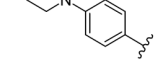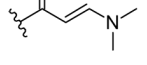
		R¹	R²	IC$_{50}$ ALK (μM)
141				0.74
142				9.3
143				>10
144				>10
145				>10
146				1.2
147				0.79
148				>10
149				0.35

Table 5. IC$_{50}$ Values (μM) of Selected 3,6-Substituted Compounds on Ba/F3 Cells

compound	IC50 Ba/F3 NPM/ALK	IC50 Ba/F3-parental	ratio[a]
91	2.0	7.0	3.5
101	1.6	5.3	3.3
102	2.8	>10	>3.6
103	0.54	1.3	2.4
105	1.6	>10	>6.3
106	5.8	>10	>1.7
107	3.5	7.3	2.1
110	1.1	0.84	0.8
111	1.1	1.9	1.7
112	2.5	2.3	0.9
113	2.0	1.1	0.6
119	2.2	2.2	1.0
120	2.2	2.8	1.3
126	4.0	3.8	1.0
147	0.36	0.48	1.3
149	0.39	2.8	7.2

[a]Calculated as IC$_{50}$ parental/IC$_{50}$ NPM-ALK cells.

crystal structure of ALK in complex with **149** was solved at <2 Å resolution; the compound binds to the protein in the active, DFG-in conformation (Figure 1E−G). The *N*-methyl-piper-azine moiety of **149** extends beyond the ATP binding pocket and toward the solvent, pointing toward charged residue Glu1210. Conversely, the azacarbazole core lies within the ATP binding pocket of ALK, forming H-bonds with the backbone atoms of the hinge region (O-Glu1197 and N-Met1199), while the dimethyl-amino group notably points toward the P-loop, which is known to control kinase inhibitor binding and specificity. Therefore, extending into this direction may confer selectivity to the compound. Interestingly, the azacarbazole ring is not in proximity of gatekeeper Leu1196, explaining the activity of this compound toward the L1196M mutant (Figures 1F and S3). Furthermore, the carbonyl group of **149** forms a direct H-bond with the catalytic Lys1150 (Figure 1F,H), and it is in close vicinity to Gly1269 of the DFG motif. As Lys1150 normally forms a salt bridge with Glu1167 of the αC-helix in the active kinase and plays a critical role in the activation of ALK,[10] this binding mode potentially impedes ALK activation.

4. CONCLUSIONS

We report here the development of novel ALK inhibitors with α-carboline core scaffold. Extensive exploration of the chemical space led to the identification of 3,6-substituted azacarbazoles endowed with submicromolar potency and good selectivity. The crystal structure of ALK in complex with one derivative indicates standard binding mode within the active site and will allow further structure-driven optimization. To this end, we note that there may be space for further elaboration of the amine moiety
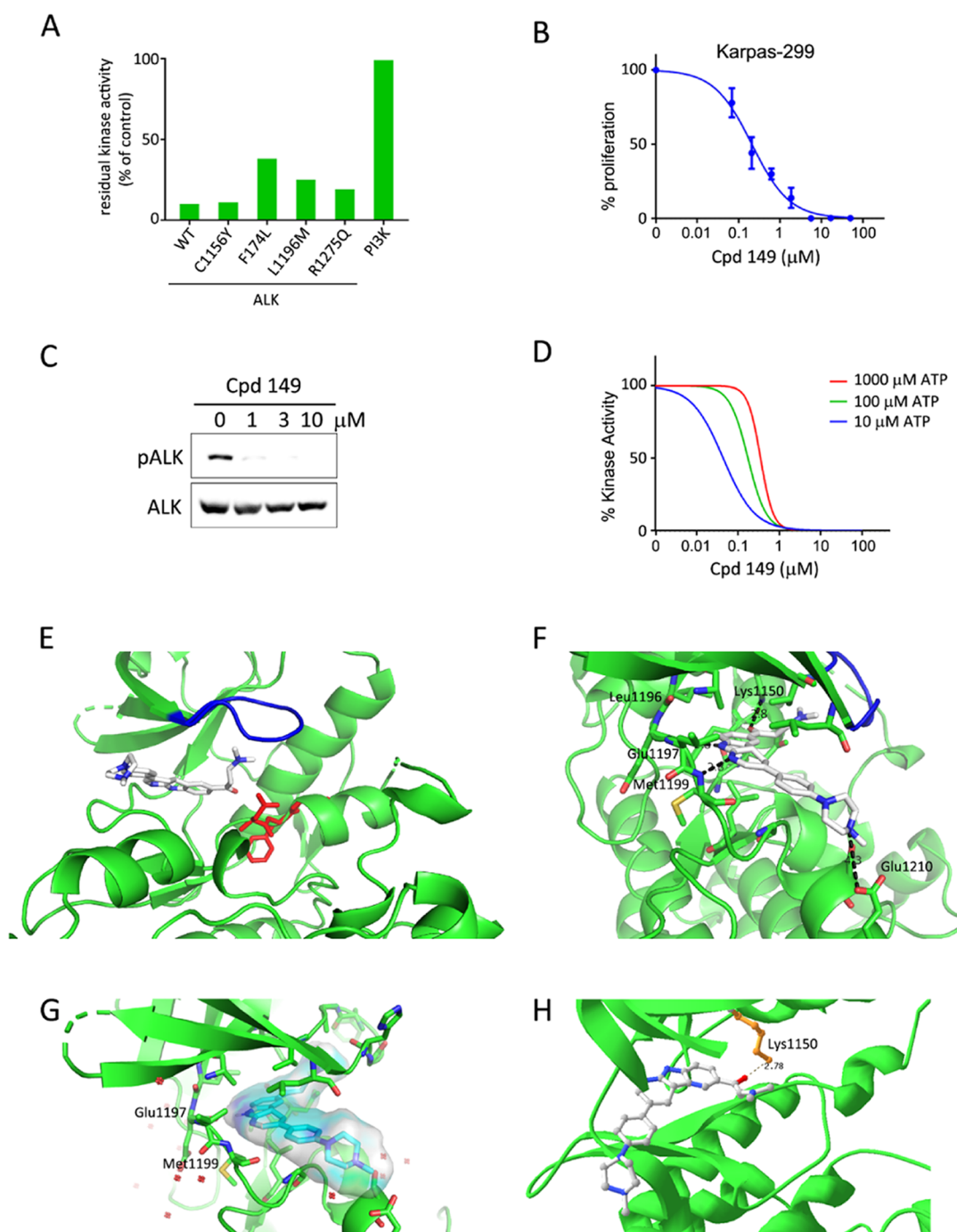
Figure 1. Characterization of compound **149**. (A) Residual *in vitro* kinase activity of the indicated kinases at 10 μM concentration of the compound, as a percent of dimethyl sulfoxide (DMSO)-treated control. (B) Dose−response curve of Karpas-299 growth inhibition by compound **149**, evaluated by thymidine incorporation assay. (C) Inhibition of NPM/ALK phosphorylation by compound **149** in Karpas-299 cells; total ALK is shown for loading control. (D) Dose−response curves of recombinant ALK inhibition by compound **149** in the presence of increasing ATP concentrations. (E) 3D structure of the **ALK:149** complex. A view of the compound binding site is shown. ALK backbone is visualized as a green ribbon, with the DFG motif colored in red and the P-loop shown in blue; compound **149** is represented in sticks. (F−H) Close-up views of the compound within the active site, with the network of interactions (dotted lines) to residues E1197, M1199, K1150, and E1210, (F) and a representation of **149** as a semitransparent molecular surface (G); red dots indicate water molecules. In panel H, the H-bond established with Lys1150 from the β3 strand of the N-terminal β-sheet is shown in greater detail.

pointing toward the P-loop to fill the pocket and establish additional interactions (Supporting Figure S4).

5. METHODS

5.1. Virtual Screening. The NCI, Specs, antimicrobial chemotherapeutics (ACD), and Maybridge databases were screened in silico for a total of over 500,000 compounds filtering for hitlike and leadlike properties (M_w < 500; $c \log P$ < 5; H-Bond donors < 5; H-Bond acceptors < 10; polar surface area < 150 Å^2) and ADME/Tox predictions. Compounds passing filters were docked using DOCK 4.0 software to published crystal structures of ALK kinase domain (PDB IDs: 3L9P, 2XB7,

Table 6. IC$_{50}$ Values (μM) Obtained with Compound 149 on ALK Mutants in a Radiometric Assay and in Cell Proliferation Assays

	ALK WT	ALK L1196M	ALK C1156Y	ALK F1174L	ALK R1275Q	Ba/F3 NPM/ ALK WT	Ba/F3 NPM/ALK L1196M	Ba/F3 NPM/ALK G1202R	Karpas-299	SUPM2
Cpd 149	0.14	0.26	0.19	0.45	0.25	0.39	0.95	7.4	0.21	0.54

3LCT, 3LCS, 2XP2, 5J7H), all in the DFG-in conformation, to account for slight differences observed in the position of the P-loop (Supporting Figure S5). Top 1000 scoring compounds were then re-docked with FlexX and GOLD, using flexible docking procedures, to validate the screening results and to confirm the docking poses. Binding affinities were estimated using five scoring functions (F-Score, PMF, D-Score, Chem-Score, G-Score) to obtain a final consensus score.[11] Compounds with high consensus scores and conserved interaction with both docking algorithms were further selected for experimental testing. 3D data were analyzed and generated by PyMOL and SYBYL.

5.2. Chemistry. The synthesis and chemical characterization of the compounds is detailed in the Supporting Material.

5.3. Biochemistry and Cell Biology. Compounds were experimentally tested using an enzyme-linked immunosorbent assay (ELISA)-based kinase assay as previously described.[8,12] Briefly, purified recombinant ALK kinase domain (aa 1073−1410), wild-type or L1196M mutant, was incubated with inhibitors and Mg^{++}-ATP in an appropriate buffer and loaded onto peptide substrate-coated wells. The reaction was run at 30 °C for 20 min. The phosphorylated peptide was then quantified by anti-phosphotyrosine antibody (clone PY20), after washing. Radiometric assays and selectivity profiling were run at ProQinase GmbH (Germany). Ba/F3 cells stably expressing NPM/ALK variants were generated by electroporation, selection with G418 (1 mg/mL), and second selection by IL3 withdrawal, as previously reported.[13] Cell proliferation was assayed by [^{3}H]-thymidine incorporation as described.[14] Dose−response curve fitting was performed by GraphPad Prism software, using nonlinear regression of normalized data. Western blotting was performed as described previously[13] using phospho-ALK (Tyr1604; #3341) and total ALK (#3633) antibodies (Cell Signaling Technology).

5.4. Crystallization and Structure Determination. Crystallization and X-ray diffraction studies were carried out at Argenta Discovery 2009 Ltd. (Harlow, U.K.). Briefly, the ALK kinase domain (aa 1093−1411 with N-terminal cleavable His6-tag) was purified from Sf9 cells by nickel affinity chromatography and crystallized by the hanging drop vapor diffusion protocol as previously described.[15] The ALK:**149** complex was obtained by soaking 2 mM compound into ALK-KD crystals. Diffraction data were collected at the Diamond synchrotron (U.K.). The coordinates file will be deposited in the PDB database and is freely available upon request to the corresponding author.

ASSOCIATED CONTENT

Supporting Information

The Supporting Information is available free of charge at https://pubs.acs.org/doi/10.1021/acsomega.2c00507.

Docking pose of two representative -carboline analogues (Figure S1); correlation between calculated and experimental activity (Figure S2); view of the ALK site (Figure S3); view of the area of potential interaction (Figure S4);

superposition of the active site residues (Figure S5); structure and activity (IC50) (Table S1); kinase selectivity profiling (Table S2); and synthetic schemes (PDF)

AUTHOR INFORMATION

Corresponding Authors

Luca Mologni − *Dept. of Medicine and Surgery, University of Milano-Bicocca, Monza 20900, Italy; Galkem srl, Monza 20900, Italy;* orcid.org/0000-0002-6365-5149; Email: luca.mologni@unimib.it

Leonardo Scapozza − *Galkem srl, Monza 20900, Italy; School of Pharmaceutical Sciences, University of Geneva, Geneva 1211, Switzerland; Institute of Pharmaceutical Sciences of Western Switzerland, University of Geneva, Geneva 1211, Switzerland;* Email: leonardo.scapozza@unige.ch

Authors

Sébastien Tardy − *Laboratoire Chimie Organique 2-Glycochimie, CNRS-Université Claude Bernard Lyon 1, Lyon 69100, France; School of Pharmaceutical Sciences, University of Geneva, Geneva 1211, Switzerland; Institute of Pharmaceutical Sciences of Western Switzerland, University of Geneva, Geneva 1211, Switzerland*

Alfonso Zambon − *Department of Chemistry and Geological Sciences, University of Modena and Reggio Emilia, Modena 41125, Italy;* orcid.org/0000-0002-8074-2308

Alexandre Orsato − *Laboratoire Chimie Organique 2-Glycochimie, CNRS-Université Claude Bernard Lyon 1, Lyon 69100, France; Department of Chemistry, Universidade Estadual de Londrina, Paraná 86057-970, Brazil;* orcid.org/0000-0001-7379-126X

William H. Bisson − *School of Pharmaceutical Sciences, University of Geneva, Geneva 1211, Switzerland; Knight Cancer Institute, Oregon Health & Science University, Portland, Oregon 97227, United States*

Monica Ceccon − *Dept. of Medicine and Surgery, University of Milano-Bicocca, Monza 20900, Italy*

Michela Viltadi − *Dept. of Medicine and Surgery, University of Milano-Bicocca, Monza 20900, Italy*

Joseph D'Attoma − *Laboratoire Chimie Organique 2-Glycochimie, CNRS-Université Claude Bernard Lyon 1, Lyon 69100, France*

Sara Pannilunghi − *School of Pharmaceutical Sciences, University of Geneva, Geneva 1211, Switzerland; Institute of Pharmaceutical Sciences of Western Switzerland, University of Geneva, Geneva 1211, Switzerland*

Vito Vece − *Dept. of Medicine and Surgery, University of Milano-Bicocca, Monza 20900, Italy; Department of Chemistry, Massachusetts Institute of Technology, Cambridge, Massachusetts 02139, United States*

Jerome Bertho − *Galkem srl, Monza 20900, Italy*

Peter Goekjian − *Galkem srl, Monza 20900, Italy; Laboratoire Chimie Organique 2-Glycochimie, CNRS-Université Claude Bernard Lyon 1, Lyon 69100, France*

Carlo Gambacorti-Passerini − *Dept. of Medicine and Surgery, University of Milano-Bicocca, Monza 20900, Italy; Galkem srl, Monza 20900, Italy*

■ ACKNOWLEDGMENTS

■ REFERENCES

(1) Sharma, G. G.; Mota, I.; Mologni, L.; Patrucco, E.; Gambacorti-Passerini, C.; Chiarle, R. Tumor Resistance against ALK Targeted Therapy-Where It Comes from and Where It Goes. *Cancers* **2018**, *10*, No. 62.

(2) Gambacorti Passerini, C.; Farina, F.; Stasia, A.; Redaelli, S.; Ceccon, M.; Mologni, L.; Messa, C.; Guerra, L.; Giudici, G.; Sala, E.; Mussolin, L.; Deeren, D.; King, M. H. H.; Steurer, M.; Ordemann, R.; Cohen, A. M. M.; Grube, M.; Bernard, L.; Chiriano, G.; Antolini, L.; Piazza, R. Crizotinib in Advanced, Chemoresistant Anaplastic Lymphoma Kinase-Positive Lymphoma Patients. *JNCI: J. Natl. Cancer Inst.* **2014**, *106*, No. djt378.

(3) Kwak, E. L.; Bang, Y. J.; Camidge, D. R.; Shaw, A. T.; Solomon, B.; Maki, R. G.; Ou, S. H.; Dezube, B. J.; Janne, P. A.; Costa, D. B.; Varella-Garcia, M.; Kim, W. H.; Lynch, T. J.; Fidias, P.; Stubbs, H.; Engelman, J. A.; Sequist, L. V.; Tan, W.; Gandhi, L.; Mino-Kenudson, M.; Wei, G. C.; Shreeve, S. M.; Ratain, M. J.; Settleman, J.; Christensen, J. G.; Haber, D. A.; Wilner, K.; Salgia, R.; Shapiro, G. I.; Clark, J. W.; Iafrate, A. J. Anaplastic Lymphoma Kinase Inhibition in Non-Small-Cell Lung Cancer. *N. Engl. J. Med.* **2010**, *363*, 1693−1703.

(4) Redaelli, S.; Ceccon, M.; Zappa, M.; Sharma, G. G.; Mastini, C.; Mauri, M.; Nigoghossian, M.; Massimino, L.; Cordani, N.; Farina, F.; Piazza, R.; Gambacorti-Passerini, C.; Mologni, L. Lorlatinib Treatment Elicits Multiple On- and Off-Target Mechanisms of Resistance in ALK-Driven Cancer. *Cancer Res.* **2018**, *78*, 6866−6880.

(5) Yoda, S.; Lin, J. J.; Lawrence, M. S.; Burke, B. J.; Friboulet, L.; Langenbucher, A.; Dardaei, L.; Prutisto-Chang, K.; Dagogo-Jack, I.; Timofeevski, S.; Hubbeling, H.; Gainor, J. F.; Ferris, L. A.; Riley, A. K.; Kattermann, K. E.; Timonina, D.; Heist, R. S.; Iafrate, A. J.; Benes, C. H.; Lennerz, J. K.; Mino-Kenudson, M.; Engelman, J. A.; Johnson, T. W.; Hata, A. N.; Shaw, A. T. Sequential ALK Inhibitors Can Select for Lorlatinib-Resistant Compound ALK Mutations in ALK-Positive Lung Cancer. *Cancer Discovery* **2018**, *8*, 714−729.

(6) Sharma, G. G.; Cortinovis, D.; Agustoni, F.; Arosio, G.; Villa, M.; Cordani, N.; Bidoli, P.; Bisson, W. H.; Pagni, F.; Piazza, R.; Gambacorti-Passerini, C.; Mologni, L. A Compound L1196M/G1202R ALK Mutation in a Patient with ALK-Positive Lung Cancer with Acquired Resistance to Brigatinib Also Confers Primary Resistance to Lorlatinib. *J. Thorac. Oncol.* **2019**, *14*, e257−e259.

(7) Gambacorti-Passerini, C.; Mologni, L.; Scapozza, L.; Ahmed, S.; Goekjian, P.; Gueyrard, D.; Popowycz, F.; Joseph, B.; Schneider, C.; Garcia, P. Alfa-carbolineInhibitors Of Npm-alk, Ret, And Bcr-abl. US8895744B22010.

(8) Mologni, L.; Sala, E.; Riva, B.; Cesaro, L.; Cazzaniga, S.; Redaelli, S.; Marin, O.; Pasquato, N.; Donella-Deana, A.; Gambacorti-Passerini,

C. Expression, Purification, and Inhibition of Human RET Tyrosine Kinase. *Protein Expression Purif.* **2005**, *41*, 177−185.

(9) Krug, M.; Wichapong, K.; Erlenkamp, G.; Sippl, W.; Schächtele, C.; Totzke, F.; Hilgeroth, A. Discovery of 4-Benzylamino-Substituted α-Carbolines as a Novel Class of Receptor Tyrosine Kinase Inhibitors. *ChemMedChem* **2011**, *6*, 63−72.

(10) Roskoski, R. J. Anaplastic Lymphoma Kinase (ALK): Structure, Oncogenic Activation, and Pharmacological Inhibition. *Pharmacol. Res.* **2013**, *68*, 68−94.

(11) Wang, R.; Lu, Y.; Wang, S. Comparative Evaluation of 11 Scoring Functions for Molecular Docking. *J. Med. Chem.* **2003**, *46*, 2287−2303.

(12) Donella-Deana, A.; Marin, O.; Cesaro, L.; Gunby, R. H.; Ferrarese, A.; Coluccia, A. M. L.; Tartari, C. J.; Mologni, L.; Scapozza, L.; Gambacorti-Passerini, C.; Pinna, L. A. Unique Substrate Specificity of Anaplastic Lymphoma Kinase (ALK): Development of Phosphoacceptor Peptides for the Assay of ALK Activity. *Biochemistry* **2005**, *44*, 8533−8542.

(13) Mologni, L.; Sala, E.; Cazzaniga, S.; Rostagno, R.; Kuoni, T.; Puttini, M.; Bain, J.; Cleris, L.; Redaelli, S.; Riva, B.; Formelli, F.; Scapozza, L.; Gambacorti-Passerini, C. Inhibition of RET Tyrosine Kinase by SU5416. *J. Mol. Endocrinol.* **2006**, *37*, 199−212.

(14) Gambacorti-Passerini, C.; Le Coutre, P.; Mologni, L.; Fanelli, M.; Bertazzoli, C.; Marchesi, E.; Di Nicola, M.; Biondi, A.; Corneo, G. M.; Belotti, D.; Pogliani, E.; Lydon, N. B. Inhibition of the ABL Kinase Activity Blocks the Proliferation of BCR/ABL+ Leukemic Cells and Induces Apoptosis. *Blood Cells, Mol., Dis.* **1997**, *23*, 380−394.

(15) Huang, Q.; Johnson, T. W.; Bailey, S.; Brooun, A.; Bunker, K. D.; Burke, B. J.; Collins, M. R.; Cook, A. S.; Cui, J. J.; Dack, K. N.; Deal, J. G.; Deng, Y.-L.; Dinh, D.; Engstrom, L. D.; He, M.; Hoffman, J.; Hoffman, R. L.; Johnson, P. S.; Kania, R. S.; Lam, H.; Lam, J. L.; Le, P. T.; Li, Q.; Lingardo, L.; Liu, W.; Lu, M. W.; McTigue, M.; Palmer, C. L.; Richardson, P. F.; Sach, N. W.; Shen, H.; Smeal, T.; Smith, G. L.; Stewart, A. E.; Timofeevski, S.; Tsaparikos, K.; Wang, H.; Zhu, H.; Zhu, J.; Zou, H. Y.; Edwards, M. P. Design of Potent and Selective Inhibitors to Overcome Clinical Anaplastic Lymphoma Kinase Mutations Resistant to Crizotinib. *J. Med. Chem.* **2014**, *57*, 1170−1187.